

Mössbauer evaluation of the interparticle magnetic Interactions within the magnetic hyperthermia beads



Mikhail Polikarpov^{a,*}, Valery Cherepanov^a, Mikhail Chuev^b, Raul Gabbasov^a, Iliya Mischenko^b, Nirmesh Jain^c, Steve Jones^d, Brian Hawkett^c, Vladislav Panchenko^a

^a National Research Centre “Kurchatov Institute”, Moscow, Russia

^b Institute of Physics and Technology, Russian Academy of Sciences, Moscow, Russia

^c Key Centre for Polymers and Colloids, University of Sydney, NSW, Australia

^d Sirtex Medical Limited, Sydney, NSW 2060, Australia

ARTICLE INFO

Article history:

Received 30 June 2014

Received in revised form

2 October 2014

Accepted 6 October 2014

Available online 30 October 2014

ABSTRACT

Mössbauer spectroscopy was used for direct experimental measurement of the Néel barrier height for magnetization reversal in ensembles of interacting γ -Fe₂O₃ nanoparticles. As the barrier height is proportional to the size of the magnetic cluster, these measurements enable an evaluation of the relative sizes of the magnetically coupled clusters that are formed during the manufacture of the magnetic hyperthermia beads. For the hyperthermia beads, which were synthesized and studied in the work, an increase in the size of the magnetically coupled cluster corresponds to a reduction of the specific loss power.

© 2014 Elsevier B.V. All rights reserved.

1. Introduction

Magnetic particle hyperthermia is today considered to be the most promising field for the therapeutic application of magnetic nanoparticles. It involves treatment of tumor cells at a temperature of 42–46 °C, which is achieved by the targeted delivery and heating of magnetic nanoparticles in an external alternating magnetic field. One such problem that prevents a widespread use of this method in clinical practice is that the heating should only occur in a local target area around the magnetic heater and leave surrounding healthy tissue unaffected. As a result of this demand, the optimal magnetic heater must be equipped with means for remote control of its temperature, or possess the ability to automatically turn off the heating if the temperature exceeds a critical value. There are two possible ways of creating such “auto off” magnetic carriers with nonlinear dependence of the electromagnetic field absorption coefficient on the temperature. The first is to search for a bulk ferromagnetic material with the Curie point lying in the 42–45 °C temperature range. The second way is based on the synthesis of superferromagnetic materials. These materials are ensembles of dipole interacting magnetic nanoparticles, with collective magnetic properties that depend on correlation bonds arising between magnetization vectors of neighboring particles [1–3]. Absorption of electromagnetic radiation in such systems

critically depends on the interparticle magnetic dipole interactions. This paper aims to study the influence of the interparticle magnetic interactions within the magnetic hyperthermia beads on their heating properties.

Depending on the construction of the magnetic bead, heat can be generated in an alternating magnetic field by different physical mechanisms. For example, in bulk conducting materials the main mechanism is resistance heating due to eddy currents. In smaller sized multidomain ferromagnetic materials, the hysteresis losses due to displacement of domain walls become dominant. In smaller single domain magnetic nanoparticles, the hysteresis losses induced by the rotation of magnetic moments inside the domains are the major mechanism. For the smallest superparamagnetic particles the magnetic heating due to Néel and Brownian relaxation processes prevails [4]. It should be mentioned that effective magnetic hyperthermia beads usually represent a more complicated nanoconstruction. Typically, they are concentrated ensembles of single domain, or superparamagnetic nanoparticles, sometimes with strong interparticle magnetic dipole interactions, enclosed in an organic matrix. As a result the heating mechanism for such composite beads becomes combined, complicating its identification.

On the other hand, such ensembles offer a unique way of engineering the magnetic response by modifying the strength of the dipolar interactions between particles. It was recently experimentally demonstrated that strongly interacting single-domain cubic iron oxide particles that resemble bacterial magnetosomes have superior magnetic heating efficiency compared to spherical

* Corresponding author.

E-mail address: polikarpov.imp@gmail.com (M. Polikarpov).

particles of similar sizes [5]. The influence of particle chain formation on the normalized heating properties of both low- (spherical) and high- (parallelepiped) anisotropy ferrite-based magnetic fluids was explored in [6]. Analysis of ferromagnetic resonance data showed that high particle concentration, which correlates with increasing chain length, leads to a decrease in the specific loss power.

Recent experiments demonstrated that the shape of the Mössbauer spectra of polymer composites based on single-domain magnetic particles depends more on an inter-particle interaction than on the superparamagnetic properties of a separate particle [7]. The asymmetric shape of lines with sharp outer and smeared inward sides proved to be the characteristic feature of the spectra of such systems with strong inter-particle interaction [7,8]. In this work this phenomenon was used in a quantitative evaluation of the magnetic interactions inside different magnetic beads, which are prepared from the same nanoparticles.

2. Materials and methods

2.1. Materials

Monoacryloxyethyl phosphate (MAEP, Aldrich) was passed through an inhibitor removal column (Aldrich) prior to use. 1,4-Dioxane (Fluka) was distilled under reduced pressure. RAFT agent 2-([butylsulfanyl]carbonothioyl)sulfanylpropanoic acid (BuPAT, DuluxGroup Australia), acrylic acid (Aldrich), methyl methacrylate (Aldrich), butyl acrylate (Aldrich) acrylamide (AAm, Aldrich), N-(isobutoxymethyl)acrylamide (Aldrich), 4,4'-azobis(4-cyanovaleric acid) (V-501, Wako), and sodium hydroxide (NaOH, Aldrich) were all used as received.

The aqueous dispersion of iron oxide nanoparticles (SB) used in this work was obtained from Sirtex Medical Limited (Sirtex NPs). Poly(Monoacryloxyethyl phosphate)₁₀-block-poly(acrylamide)₃₅-N-(isobutoxymethyl)acrylamide)₃ macro-RAFT was prepared as reported previously [9]. Sterically stabilized iron oxide nanoparticles (NJ), based on the Sirtex NPs, were synthesized in water as reported previously [10].

2.2. Preparation of hyperthermia beads

Hyperthermia beads were prepared in two different ways.

2.2.1. Preparation of beads (EP-73)

1 g of the sterically stabilized ferrofluid (55 wt%) was taken in a 10 ml Scintillation vial. 100 g, 2 wt% solution of oil soluble surfactant, Span80 in toluene was separately prepared in a 100 ml beaker. 2 g of this surfactant solution was then added to the scintillation vial containing ferrofluid. The mixture in the scintillation vial was emulsified on a vortex mixer for about 1 min. The emulsion was then added to the surfactant solution in a 250 ml round bottom flask. The solution in the round bottom flask was stirred mechanically. The flask was then heated slowly to the reflux temperature (110 °C) of toluene. Water from the emulsion drops was stripped off along with toluene in the form of an azeotrope leaving dry microspheres in the continuous phase. Toluene was decanted from the mixture as microspheres precipitated under gravity. Microspheres were then washed twice with acetone to remove any left over toluene and Span80 surfactant. At the end of this step the microspheres are in the form of a dry powder. Dry microspheres were then cured at 180 °C in a heating oven for about 2 h. This resulted in the crosslinking of polymer molecules stabilizing the iron oxide nanoparticles within the microspheres. The beads had an average particle size of 35 μm as determined by light microscopy. The micro-beads contain about

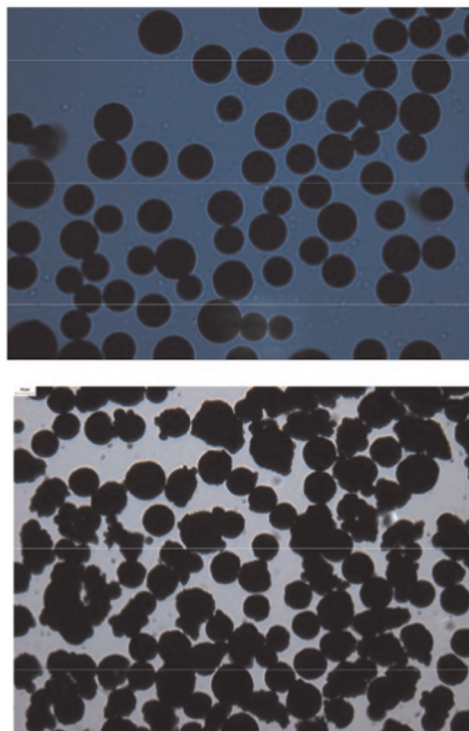


Fig. 1. Micrographs of 35-μm diameter spherical beads (EP-73) and the beads with uneven surfaces (EP-72).

10^9 particles per bead. This approach to making beads yields smooth spherical beads (Fig. 1), which contain about 77% of γ -Fe₂O₃ by weight.

2.2.2. Preparation of beads (EP-72)

The particles used in these beads were sterically stabilized with a poly (acrylic acid)₁₀-block-poly(methyl methacrylates)₁₀ macro-RAFT. The sterically stabilized particles were then dispersed in methyl methacrylate monomer. Microspheres were prepared by suspension polymerization of the methyl methacrylate based ferrofluid in water. The micro-beads contain about 10^9 particles per bead. This approach to making beads yields beads (Fig. 1) with uneven surface. The beads contained about 79% of γ -Fe₂O₃.

2.3. Heat generation

Heating was measured using a self made magnetic coil. The magnetic field was generated using a Hewlett-Packard 3324A synthesized function/sweep generator with an 1140LA power amplifier. The amplitude of the magnetic field that is used for the heating experiment is 90 Oe and the experiments were carried out at a frequency of 100 kHz. Samples for heating experiments were prepared according to the following procedure: approximately 0.05 g of material (solid beads) was added to a vial and then approximately 1.5 ml of hot agar was added. The sample was shaken to provide a uniform suspension of beads once the agar had set. The sample was cooled at room temperature for at least an hour to allow the agar to set before the sample was heated. The samples prepared were placed in the magnetic coil and the temperature increase was measured using a luxtron m3300 fluoroptic thermometer. The temperature of the samples was measured for 1 min prior to turning on the magnetic field and then for 2 min once the field was activated. It was found that the samples generate very different amounts of heat when exposed to the same oscillating magnetic field. The bead (EP-72) produced heating at 9.13 W/g or

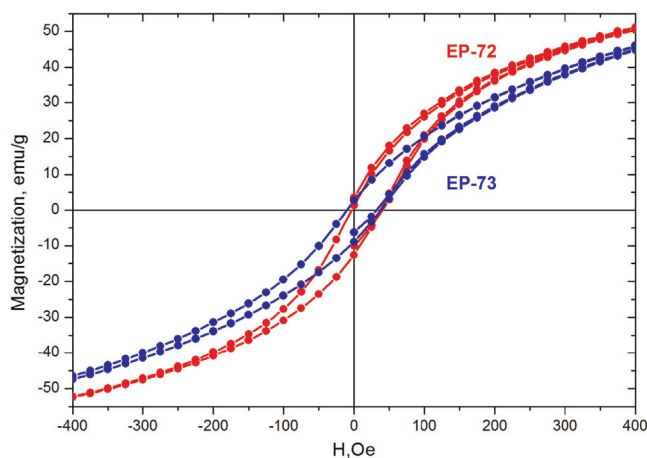


Fig. 2. The magnetization curves of the (EP-72) и (EP-73) samples.

20 W/cm³, and the bead (EP-73) produced heating at 0.85 W/g or 1.7 W/cm³.

2.4. Magnetization curves

In the case of a time-varying field, it is generally recognized that the area under the hysteresis loop is related to the amount of heat generated per cycle. The measurement of the magnetization curves of the two beads (EP-72) and (EP-73) was carried out. The samples were prepared by drying the starting ferrofluids to a powder at a temperature of 60 °C. Magnetization curves were measured on the vibrating sample magnetometer at room temperature. The measurements were carried out with a constant step 25 Oe of the magnetic field up to 1 kOe. Fig. 2 shows the magnetization curves. Samples (EP-72) and (EP-73) show remanences of about 11 emu/g and about 6 emu/g respectively. It should be noted that the areas of the hysteresis loops for two samples have roughly the same magnitude. Point-to-point calculation gives 3373 emu/g Oe for (EP-73) and 2568 emu/g Oe for (EP-72). Thus, sample (EP-73) has about a 25% larger hysteresis loop than (EP-72), despite the lower heat production.

2.5. Samples

Four types of the dried samples were prepared for the further study of the interparticle magnetic dipole interactions (Table 1). All the samples are prepared on the base of the same 25 nm diameter ferrimagnetic nanoparticles γ -Fe₂O₃ and differ only in the way of their connection to the magnetic ensemble. They include the nanoparticles in the intrinsic electrostatically stabilized ferrofluid (SB) and in the sterically stabilized ferrofluid (NJ) and two

Table 1
Summary of characteristics of the samples.

| Sample | (SB) | (NJ) | (EP-72) | (EP-73) |
|--|------|------|---------|-----------|
| Preparation | | | | |
| Nanoparticles γ -Fe ₂ O ₃ ~25 nm | + | + | + | + |
| Electrostatic stabilization in water | + | + | + | + |
| Steric stabilization in water | - | + | + | + |
| Polymer beads ~35 μ m, containing ~10 ⁹ nanoparticles | - | - | + | + |
| Characterization | | | | |
| Shape of the beads | - | - | Uneven | Spherical |
| γ -Fe ₂ O ₃ per bead (wt) | - | - | 79% | 77% |
| Heat generation (W/g) | - | - | 9.13 | 0.85 |
| Area of the hysteresis loop (emu/g Oe) | - | - | 2568 | 3373 |

samples of magnetic hyperthermia beads (EP-72) and (EP-73), contained 79% and 77% of the same nanoparticles, respectively.

The base (SB) ferrofluid is stabilized electrostatically. The stabilizing electric double layer exists under appropriate conditions of pH only. So, the magnetic iron oxide particles have to aggregate and contact with each other after drying.

The particles in the sterically stabilized ferrofluid (NJ) are individually coated with a short poly (acrylic acid)-b-poly (acrylamide) copolymer, designed to form the thinnest possible layer while remaining strongly attached to the iron oxide surface over a wide range of nanoparticle concentrations. Thermogravimetric analysis yields an iron oxide content in the dried particles, consistent with dry polymer coating of approximately 1 nm in thickness. So, if we dried the sterically stabilized particles, a very thin layer of polymer would still separate them.

The hyperthermia beads (EP-72) and (EP-73) are prepared from the sterically stabilized ferrofluid (NJ). The beads are prepared by polymerization of sterically stabilized ferrofluid (NJ). They are stable to drying and contain about 10⁹ particles per one 35- μ m diameter bead.

3. Mössbauer study of the interparticle interactions

3.1. physical basis of the method of mössbauer relaxation spectroscopy

The magnetization vector of the superparamagnetic nanoparticle can spontaneously reverse their orientation due to a coherent rotation of all individual spins in the particle. The relaxation time is given by the Néel equation [11]

$$\tau = \tau_0 \exp(KV/k_bT) \quad (1)$$

where K is the magnetic anisotropy constant, V is the particle volume, k_b is Boltzmann's constant, T is the temperature. The typical time of the reverse in iron oxide nanoparticles is about 10⁻⁶-10⁻¹⁰ s in the temperature range 77-300 K. The results obtained from the investigation of the magnetic properties of these superparamagnetic particles depend on a correlation between the time of observation and that of magnetization vector relaxation. If the time of observation is much less than that of relaxation then the magnetization vector keeps its direction constant during the time of measurement and the particles exhibit ferromagnetic properties. In the opposite case the magnetization vector manages to reverse its direction during the time of measurement. As a result an average value of the magnetic moment during the time of observation becomes zero and the particles appear as a paramagnetic substance. The measurement time in Mössbauer spectroscopy, which is determined by the lifetime of the excited state of the ⁵⁷Fe nucleus, is 10⁻⁸ s. As a result, the Mössbauer spectrum of magnetic nanoparticles may look as a magnetic sextet of lines for particles with slowly oscillating magnetization vectors or a paramagnetic doublet of lines for particles with fast oscillating magnetization vectors. For the individual superparamagnetic nanoparticle the oscillation frequency depends on its size and temperature. As a result the shape of the Mössbauer spectrum may gradually changes from the sextet to the doublet of lines, thus enabling to study the relaxation phenomena. The frequency of the oscillation in the ensemble of superparamagnetic particles can be additionally changed by the establishment of correlation bonds between magnetization vectors of neighboring particles. This is the so-called superferromagnetic state [7]. It should be noted that the parameters K and V in the Eq. (1) lose their meaning when describing relaxation in such system. This is due to the uncertainty of the real dimensions of the cluster of

nanoparticles, which are connected by the magnetic dipole interaction. Therefore the Néel equation for the relaxation time of magnetization vector in the superferromagnetic cluster can be written as

$$\tau = \tau_0 \exp(E_b/k_b T) \quad (2)$$

where E_b is the barrier height that the magnetization vector has to overcome in order to reverse its orientation in the cluster. One of the main signs of the establishment of such state is the asymmetric shape of the lines on the Mössbauer spectra with sharp outer and smeared inward sides [7,8].

The theory of magnetism for ferrimagnetic nanoparticles is still at the development stage. In ferrimagnetic identical atoms occupying different crystallographic positions form two interleaved magnetic sublattices with their own magnetic moments and the particle energy depends on the orientation of both moments relative to the easy axis. However, on deviation of the sublattice moments from mutually opposite directions, the system energy increases sharply – that is the energy profile of the ferrimagnetic particle appears to be nearly one-dimensional as for a ferromagnetic particle. It offers a possibility to regard a spectrum of ferrimagnetic particles in the first approximation as a sum of two ferromagnetic contributions from each of the sublattices with their own hyperfine parameters and a common diffusion constant characterizing the joint relaxation process intensity [12]. In this approximation the spectrum of γ -Fe₂O₃ particles contains two components with slightly smaller isomer shifts than those of the A and B sites in bulk material, which can be treated within the same ferromagnetic approach.

In the presented work for the interpretation of the experimental Mössbauer spectra, we carried out the simultaneous mean-square analysis for the whole set of spectra in the two-sublattices approximation on the base of multi-level relaxation model [13] of magnetic dynamics for each sublattice using Anderson's stochastic approach [14] to calculate the spectra in the presence of combined magnetic and quadrupolar hyperfine interaction [15].

3.2. Experimental results

Mössbauer spectra were measured at the temperatures 77–300 K with an electro-dynamic spectrometer MS-1104Em, working in the constant acceleration mode. ⁵⁷Co in a rhodium matrix of 5 mCi activity was used as a source of gamma-radiation. The isomer shifts were determined in relation to the absorption line of α -Fe.

Fig. 3 shows the typical Mössbauer spectra of the γ -Fe₂O₃ particles, measured in the sample of the sterically stabilized ferrofluid (NJ) and in the sample of poor heating micro-bead (EP-73), obtained from this ferrofluid by polymerization. Vertical sizes of the markers on the curves indicate experimental errors (doubled standard deviation). Solid lines represent theoretical spectra. At liquid nitrogen temperature both spectra look almost identical. The weak asymmetry of the spectral lines may be caused by both the two-sublattices magnetic structure of the γ -Fe₂O₃ and the presence of magnetic relaxation. At room temperature the smearing of the inward sides of the lines of the Mössbauer spectra of both samples increases. This reveals the relaxation mechanism of the lines broadening and indicates presence of the dipole interparticle interactions in both samples. It is seen that with increasing temperature the asymmetry of spectral lines of sterically stabilized particles (NJ) increases faster than the asymmetry for the (EP-73) sample.

The Mössbauer absorption spectra of samples (SB) and (EP-72) proved to be qualitatively similar to the spectra of (NJ) and (EP-73) and differ only by the asymmetry. Their experimental points lie in

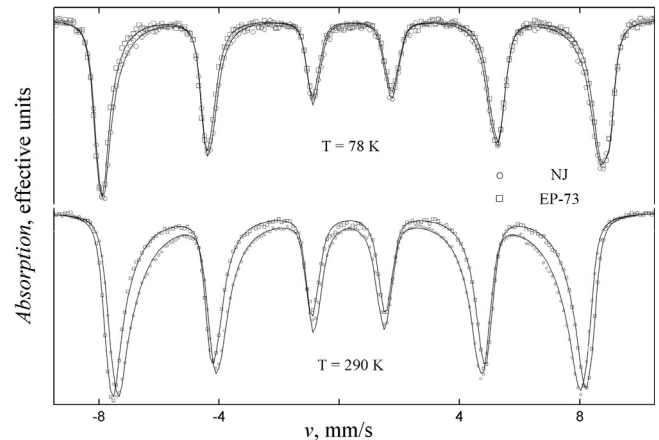


Fig. 3. ⁵⁷Fe Mössbauer absorption spectra (markers) measured at liquid nitrogen and at room temperature for the samples (NJ) and (EP-73) containing the same magnetic nanoparticles in different environments. All measurements are brought to the same absorption effect for the ease of comparison. Vertical sizes of the markers on the curves indicate experimental errors (doubled standard deviation). Solid lines represent theoretical spectra.

the interval between the spectra of the samples (NJ) and (EP-73) in the Fig. 3. Fig. 4 shows on an enlarged scale the first (leftmost) line of the spectra for the samples (NJ), (SB), (EP-72), (EP-73) superimposed on each other. All spectra are brought to the same absorption effect for the ease of comparison. Vertical sizes of the markers on the curves indicate experimental errors (doubled standard deviation). Solid lines represent theoretical spectra. The asymmetric shape of the lines on all Mössbauer spectra confirms the presence of interparticle dipole interactions in all the samples. It is seen that with increasing temperature the asymmetry and smearing of the inward sides of spectral lines increases, that indicates the presence of magnetic relaxation. Numerical fitting of the experimental spectra was carried out on the base of multi-level relaxation model of magnetic dynamics for two sublattices. It can be seen that the theoretical curves precisely enough describe the experimental spectra for all samples.

Table 2 shows the parameters of the hyperfine structure of the spectra, the left line of which is shown in Fig. 4. These parameters were obtained as a result of self-consistent numerical fitting of the entire group of the experimental spectra, measured for each

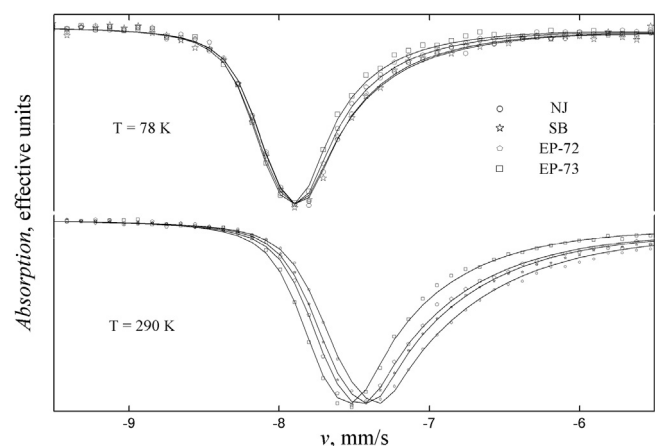


Fig. 4. The first (leftmost) lines of the ⁵⁷Fe Mössbauer absorption spectra (markers) measured at liquid nitrogen and at room temperature for the series of samples (NJ), (SB), (EP-72), (EP-73) containing the same magnetic nanoparticles in different environments. All measurements are brought to the same absorption effect for the ease of comparison. Vertical sizes of the markers on the curves indicate experimental errors (doubled standard deviation). Solid lines represent theoretical spectra.

Table 2

Mössbauer parameters, corresponding to the spectra of magnetic hyperthermia micro-beads (EP-73), (EP-73) and ensembles of base nanoparticles (SB) and sterically stabilized nanoparticles (NJ), shown in Figs. 3 and 4: $\delta_{A,B}$, isomer shift, $q_{A,B}$, quadrupolar splitting, $H_{hf,A,B}$, hyperfine field for the ferrimagnetic sublattices A and B, D , diffusion constant, E_b , energy barrier, γ_d , relative width of Gaussian distribution of nanoparticles over their diameters.

| T: All | Sample | All | | | |
|---------|-------------------|------------|-----------|-----------|-----------|
| | γ_d | 0.189 (3) | | | |
| | $-q_A$ (mm/s) | 0.208 (5) | | | |
| | $-q_B$ (mm/s) | 0.256 (2) | | | |
| | D (mm/s) | 0.0027 (2) | | | |
| T=78 K | Sample | (NJ) | (SB) | (EP-72) | (EP-73) |
| | E_b (K) | 730 (10) | 690 (10) | 840 (20) | 950 (20) |
| | $H_{hf, A}$ (kOe) | 520.5 (4) | 521.9 (4) | 519.2 (3) | 520.9 (3) |
| | $H_{hf, B}$ (kOe) | 526.6 (3) | 527.6 (3) | 526.6 (2) | 527.2 (3) |
| | δ_A (mm/s) | 0.288 (5) | 0.284 (5) | 0.290 (4) | 0.295 (5) |
| | δ_B (mm/s) | 0.524 (2) | 0.526 (3) | 0.514 (2) | 0.511 (2) |
| T=290 K | Sample | NJ | SB | EP-72 | EP-73 |
| | E_b (K) | 1340 (10) | 1490 (10) | 1550 (10) | 1900 (20) |
| | $H_{hf, A}$ (kOe) | 489.9 (2) | 493.2 (2) | 495.0 (3) | 497.6 (2) |
| | $H_{hf, B}$ (kOe) | 490.5 (1) | 493.7 (1) | 495.6 (2) | 499.2 (2) |
| | δ_A (mm/s) | 0.155 (2) | 0.177 (2) | 0.197 (3) | 0.194 (3) |
| | δ_B (mm/s) | 0.412 (1) | 0.407 (1) | 0.396 (2) | 0.395 (2) |

sample at 77, 200 (not shown), and 290 K, within the model [15]. In this procedure, it was assumed that the isomer shift $\delta_{A,B}$, quadrupolar splitting $q_{A,B}$, diffusion constant D and relative width of Gaussian distribution of nanoparticles over their diameters γ_d for all samples are the same, as they consist of the same nanoparticles. As a result the E_b parameter was determined from the numerical fitting of the experimental spectra. E_b is connected with the Néel formula for relaxation of the magnetization vector of a superferromagnetic cluster and is proportional to the barrier height that the magnetization vector has to overcome in order to reverse its orientation. For the (SB) sample the barrier height $E_b = 1490(10)$ K and for the (NJ) sample $E_b = 1340(10)$ K at room temperature. Therefore the steric stabilization results in a 10% reduction in the Néel barrier height. Besides E_b parameter proved to be 1550 (10) K for good heating bead (EP-72) and 1900 (20) K for bad heating bead (EP-73) at room temperature.

4. Discussion of results

Magnetic hyperthermia beads usually have a two-level magnetic structure. The lower level of the magnetic structure comprises single domain magnetic nanoparticles with sizes 5–35 nm with uniaxial magnetic anisotropy. In accordance with the Stoner–Wohlfarth model, the magnetization vector of such particles can spontaneously take two opposite directions (parallel or anti-parallel to the easy magnetization axis) as a result of coherent rotation of all the spins of the magnetic atoms of the nanoparticles. These two states correspond to the energy minima of the

quantum system and are separated by an energy barrier that can be overcome by thermal energy. The probability of thermal reversal of the magnetization vector in such a particle, depending on the temperature, is defined by the Néel formula (1), where the magnetic anisotropy constant K does not depend on the size V of nanoparticles and is determined only by magnetic crystal structure of the magnetic material. The second level of the magnetic structure is a concentrated ensemble of such Neel nanoparticles inside the magnetic bead. Interparticle dipole magnetic interactions between the magnetization vectors of neighboring particles alter the relaxation properties of the initial nanoparticles. Today there are no accepted methods for the phenomenological description of relaxation in such magnetically coupled clusters. The vast majority of experimentalists in interpreting the interaction effects are trying to modify the classical Néel formula for isolated superparamagnetic particle (1) by introducing to it the some modified parameters $K_{cluster}$ and $V_{cluster}$. Unfortunately, the experimental methods for measuring of these parameters do not exist. The principal advantage of the Mossbauer spectroscopy is the possibility of direct experimental measurements of the barrier height E_b in the studied ensemble of magnetic nanoparticles. E_b corresponds to the multiplication of these two parameters and has a clear physical meaning. Only this parameter allows quantitative and physically correct characterization of the influence of interparticle interactions of magnetic nanoparticles on their magnetic dynamics. The height of the barrier is directly proportional to the size of magnetic nanoparticle clusters, which determines the observed Néel relaxation. The barrier height increases with the increasing the size of the clusters, resulting, in the limiting case, in stopping the relaxation process. The minimum height of the barrier corresponds to a single isolated magnetic nanoparticle.

Today there is no theoretical model that allows the height of the Neel barrier in the interacting ensemble to be related to the amount of superparamagnetic nanoparticles in a magnetic cluster. Nevertheless, the possibility of a comparative evaluation of the sizes of magnetic clusters exists even today [16].

The value of the Neel barrier, measured in the initial ferrofluid (SB) was 1490 K. The steric stabilization has led to a decrease in the magnitude of the Neel barrier to 1340 K (NJ). Obviously, the iron oxide nanoparticles themselves, as a result of such a process cannot be changed. Therefore it can be concluded that the original ferrofluid does not contain separate nanoparticles, but their clusters (Fig. 5, SB). Steric stabilization separated the nanoparticles within the clusters and the Néel barrier of the system decreased (Fig. 5, NJ). Synthesis of the magnetic hyperthermia beads from these sterically stabilized nanoparticles leads to the formation of new magnetic clusters. The values of the Néel barriers, equal to 1550 K for the EP-72 and 1900 K for EP-73, clearly shows that the size of the magnetic clusters in EP-73 are larger than in EP-72, and both are larger than the clusters in the intrinsic ferrofluid (Fig. 5, EP72 and EP73). It turned out that in our hyperthermia beads, an

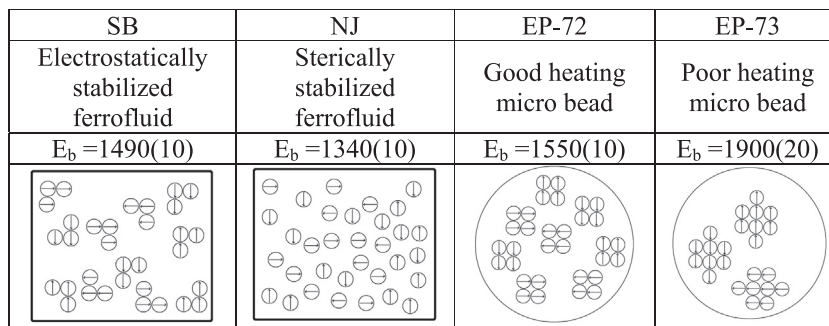


Fig. 5. Schematic illustration of relative sizes of interacting magnetic clusters in the investigated samples of ferrofluids and microbeads.

increase in the size of magnetically coupled cluster corresponds to a reduction of the specific loss power. The authors are not ready to discuss the mechanism of the influence of the magnetic cluster size on the heating capacity of the ball. Nevertheless, the observed inverse relationship of these parameters is in qualitative agreement with the conclusions made in the [6].

5. Conclusion

Mössbauer spectroscopy enables to measure the energy barrier height for the magnetization vector reversal in the cluster of interacting magnetic nanoparticles. As the barrier height is proportional to the magnetic cluster size, these measurements provide a measure of the relative sizes of the magnetic clusters that may be formed in the concentrated ensemble of the magnetic nanoparticle.

Acknowledgment

This work is supported in part by the Russian Foundation for Basic Research under Grant 13-02-12462 and by Sirtex Medical Limited.

References

- [1] M. Varon, et al., *Sci. Rep.* 3 (2013) 1234. <http://dx.doi.org/10.1038/srep01234>.
- [2] J.F. Banfield, et al., *Science* 289 (2000) 751.
- [3] S. Mørup, M.F. Hansen, C. Frandsen, J. Beilstein, *Nanotechnology* 1 (2010) 182–190.
- [4] D. Ortega, Q.A. Pankhurst, *Nanoscience* 1 (2013) 60–88. <http://dx.doi.org/10.1039/9781849734844-00060>.
- [5] C. Martinez-Boubeta, et al., *Sci. Rep.* 3 (2013) 1652. <http://dx.doi.org/10.1038/srep01652>.
- [6] L.C. Branquinho, et al., *Sci. Rep.* 3 (2013) 2887. <http://dx.doi.org/10.1038/srep02887>.
- [7] M. Polikarpov, V. Cherepanov, M. Chuev, S. Shishkov, S. Yakimov, *J. Phys.: Conf. Ser.* 217 (2010) 012114.
- [8] S. Mørup, M.F. Hansen, C. Frandsen, J. Beilstein, *Nanotechnology* 1 (2010) 182–190. <http://dx.doi.org/10.3762/bjnano.1.22>.
- [9] N.S. Bryce, et al., *Biomater. Sci.* 1 (2013) 1260.
- [10] N. Jain, Y. Wang, S.K. Jones, B.S. Hawkett, G.G. Warr, *Langmuir* 26 (2010) 4465.
- [11] L. Néel, *Ann. Geophys.* 5 (1949) 99–136.
- [12] M.A. Chuev, *JETP Lett.* 98 (8) (2013) 465–470.
- [13] D.H. Jones, K.K.P. Srivastava, *Phys. Rev. B* 34 (1986) 7542–7548.
- [14] P.W. Anderson, *J. Phys. Soc. Jpn.* 9 (1954) 316–339.
- [15] M.A. Chuev, *J. Phys.: Condens. Matter* 23 (2011) 426003 11 pp..
- [16] R.R. Gabbasov, et al., *Hyperfine Interact.* 206 (2012) 71–74.